AGU PUBLICATIONS

JGR

Journal of Geophysical Research: Planets

INTRODUCTION TO A SPECIAL SECTION

10.1002/2016JE005200

Special Section:
The Mars Science Laboratory Rover Mission (Curiosity) at The Kimberley, Gale Crater, Mars

Key Points:
- Mars Science Laboratory explored the Kimberley waypoint from sols 571–634 using its full science instrument payload
- The stratigraphic sequence most likely formed at the margins of a lake within Gale crater, prior to the existence of Mount Sharp
- The sediments at the Kimberley were derived from several igneous sources, including an alkali feldspar protolith

Supporting Information:
- Supporting Information S1
- Table S1

Correspondence to:
M. S. Rice,
melissa.rice@wwu.edu

Citation:
Rice, M. S., et al. (2017), Geologic overview of the Mars Science Laboratory rover mission at the Kimberley, Gale crater, Mars, *J. Geophys. Res. Planets*, *122*, 2–20, doi:10.1002/2016JE005200.

Received 13 OCT 2016
Accepted 30 NOV 2016
Accepted article online 22 DEC 2016
Published online 28 JAN 2017

Geologic overview of the Mars Science Laboratory rover mission at the Kimberley, Gale crater, Mars

Melissa S. Rice[1], Sanjeev Gupta[2], Allan H. Treiman[3], Kathryn M. Stack[4], Fred Calef[4], Lauren A. Edgar[5], John Grotzinger[6], Nina Lanza[7], Laetitia Le Deit[8], Jeremie Lasue[9], Kirsten L. Siebach[10], Ashwin Vasavada[4], Roger C. Wiens[7], and Joshua Williams[1]

[1]Geology Department, Western Washington University, Bellingham, Washington, USA, [2]Department of Earth Science and Engineering, Imperial College London, London, UK, [3]Lunar and Planetary Institute, Houston, Texas, USA, [4]Jet Propulsion Laboratory, California Institute of Technology, Pasadena, California, USA, [5]Astrogeology Science Center, U.S. Geological Survey, Flagstaff, Arizona, USA, [6]Division of Geological and Planetary Sciences, California Institute of Technology, Pasadena, California, USA, [7]Space Remote Sensing, Los Alamos National Laboratory, Los Alamos, New Mexico, USA, [8]Laboratoire de Planétologie et Géodynamique, Université de Nantes, Nantes, France, [9]Institut de Recherche en Astrophysique et Planétologie, Observatoire Midi-Pyrénées, CNRS, Toulouse, France, [10]Department of Geosciences, Stony Brook University, Stony Brook, New York, USA

Abstract The Mars Science Laboratory (MSL) Curiosity rover completed a detailed investigation at the Kimberley waypoint within Gale crater from sols 571–634 using its full science instrument payload. From orbital images examined early in the Curiosity mission, the Kimberley region had been identified as a high-priority science target based on its clear stratigraphic relationships in a layered sedimentary sequence that had been exposed by differential erosion. Observations of the stratigraphic sequence at the Kimberley made by Curiosity are consistent with deposition in a prograding, fluvio-deltaic system during the late Noachian to early Hesperian, prior to the existence of most of Mount Sharp. Geochemical and mineralogic analyses suggest that sediment deposition likely took place under cold conditions with relatively low water-to-rock ratios. Based on elevated K_2O abundances throughout the Kimberley formation, an alkali feldspar protolith is likely one of several igneous sources from which the sediments were derived. After deposition, the rocks underwent multiple episodes of diagenetic alteration with different aqueous chemistries and redox conditions, as evidenced by the presence of Ca-sulfate veins, Mn-oxide fracture fills, and erosion-resistant nodules. More recently, the Kimberley has been subject to significant aeolian abrasion and removal of sediments to create modern topography that slopes away from Mount Sharp, a process that has continued to the present day.

1. Introduction

The search for habitable environments on Mars requires integrated observations of stratigraphy, sedimentology, geochemistry, mineralogy, geomorphology, isotopic ratios, and organic compounds to unravel past environmental conditions. The Mars Science Laboratory (MSL) Curiosity payload [*Grotzinger et al*., 2012] is uniquely qualified to perform such an integrative investigation. Early in the mission the rover successfully characterized the habitability of an ancient, shallow lacustrine system in Gale crater at Yellowknife Bay [*Grotzinger et al*., 2014]. At this location, Curiosity detected organic molecules preserved in the Cumberland drill sample within the Sheepbed mudstone [*Freissinet et al*., 2015], which had been deposited in moderate to neutral-pH waters with low salinity and variable redox states, indicating an environment that could have been habitable to chemoautotrophic microorganisms [*Grotzinger*, 2014]. (The names Yellowknife Bay, Cumberland, Sheepbed, and other names assigned to rock targets and waypoints are informal [e.g., *Vasavada et al*., 2014]). Geochemical observations show that Yellowknife Bay rocks were derived from basaltic sources and that postdepositional aqueous alteration took place under arid and possibly cold paleoclimates [*McLennan et al*., 2014]. The young cosmogenic exposure age of the Sheepbed mudstone, combined with its location at the base of a retreating scarp in the overlying Gillespie sandstone, suggests that the organics in the Cumberland sample had been protected from degradation by high-energy radiation until the overlying outcrop was removed relatively recently (~80 Ma) by erosion [*Farley et al*., 2014].

The successful characterization of habitability and identification of organic compounds at Yellowknife Bay led the Curiosity team to adopt a sampling strategy to target rocks with minimal surface exposure ages and therefore greater potential for preserving organic material during the next phase of the mission [*Vasavada*

et al., 2014]. After leaving Yellowknife Bay, Curiosity drove southwest toward Aeolis Mons (informally called "Mount Sharp," a ~5 km high mound of sedimentary rock) across the Bradbury Rise area of Aeolis Palus (the plains surrounding Aeolis Mons), along a path called the "Rapid Transit Route" (RTR) that offered the fastest progress across safely traversable terrain [*Vasavada et al*., 2014]. Along the RTR, Curiosity stopped to perform in situ analyses at three "waypoints," informally named Darwin, Cooperstown, and the Kimberley (Figure 1a). These waypoints were selected from orbital images as locations near the planned traverse that had clear exposures of Aeolis Palus stratigraphy [*Vasavada et al*., 2014; *Stack et al*., 2016].

To expedite the arrival at Mount Sharp, the MSL team agreed to consider drilling at only one of these three waypoints. The Kimberley was selected for a drill campaign based on its clear stratigraphic relationships in a layered sedimentary sequence that had been exposed by differential erosion (Figure 1c). In images from the High-Resolution Imaging Science Experiment (HiRISE) camera on board the Mars Reconnaissance Orbiter, some outcrops exposed at the Kimberley and distributed in patches over an ~8 km^2 area of the crater floor were observed to contain regularly spaced, northeast-southwest oriented striations that had not been encountered previously on Aeolis Palus [*Stack et al*., 2016]. This enigmatic unit has been termed the Orbital Striated Outcrop (OSO), and the striations show a remarkable consistency in their strike direction across the ~8 km^2 area over which the unit is exposed [*Grotzinger et al*., 2015]. At the Kimberley, an exposure of OSO crops out beneath a light-toned, scarp- and butte-forming unit termed the Rugged Unit (RT), which was in contact with a darker-toned unit with undulating topography termed the Hummocky Plains Unit (HP) [*Stack et al*., 2016] (Table 1). A prominent scarp in the RT unit was observed in the same orientation as the active Sheepbed-Gillespie scarp in Yellowknife Bay (~152° clockwise from north; Figure 1b), and the underlying OSO appeared less dusty than surrounding outcrops (as indicated by relatively bluer hues in the HiRISE infrared-red-blue (IRB) false-color images [*Delamere et al*., 2010]); together, these observations suggested that scarps in the RT could be actively eroding and exposing relatively fresh surfaces. Therefore, the Kimberley offered an excellent opportunity to test the sampling strategy developed at Yellowknife Bay and to continue the characterization of habitability and search for organic molecules within sedimentary rocks at Gale crater.

Curiosity approached the Kimberley waypoint and performed initial reconnaissance during sols 535–570, surveyed and characterized the units at the Kimberley during sols 571–609, completed a drilling and sampling campaign at the target Windjana during sols 610–629, and departed the Kimberley during sols 630–634. Key results of the rover's geologic investigation during these periods are presented in this special section of *Journal of Geophysical Research-Planets* [*Le Deit et al*., 2016; *Lasue et al*., 2016; *Litvak et al*., 2016; *Mangold et al*., 2016; *Thompson et al*., 2016; *Treiman et al*., 2016; *Vasconcelos et al*., 2016] and elsewhere [e.g., *Grotzinger et al*., 2015; *Lanza et al*., 2016]. This introduction provides the context for specific findings at the Kimberley and integrates them together into a broader understanding of the geologic history and past habitability of Gale crater. In the following sections, we present an overview of the science campaign at the Kimberley and summary of key observations (section 2); implications for depositional environments (section 3) and sediment provenance (section 4); the history of diagenetic alteration (section 5); ongoing erosion and landscape evolution (section 6); and conclusions and implications for habitability (section 7). Although Curiosity also performed a suite of environmental monitoring and atmospheric characterization experiments at the Kimberley, the work presented here only includes results from the geological investigation.

2. Overview of the Kimberley Campaign

2.1. Naming Conventions

Prior to Curiosity's landing, the science team created a geologic map of the MSL landing ellipse, consisting of one hundred forty 1.5 × 1.5 km (0.025°) quadrangles [*Calef et al*., 2013; *Grotzinger*, 2014]. The Kimberley waypoint was informally named for the Kimberley quadrangle in which it falls, which in turn takes its name from the northernmost region of Western Australia, the site of many important geologic investigations of Precambrian rocks [e.g., *Dow and Gemuts*, 1969; *Tyler et al*., 2012, and references therein]. Note that we use "the Kimberley" instead of "Kimberley" for consistency with the Australian convention. Within the Kimberley quadrangle at Gale crater, informal science target names have been derived from rock formation names and local geographic names from the Kimberley, Western Australia. The names for Gale crater, Aeolis

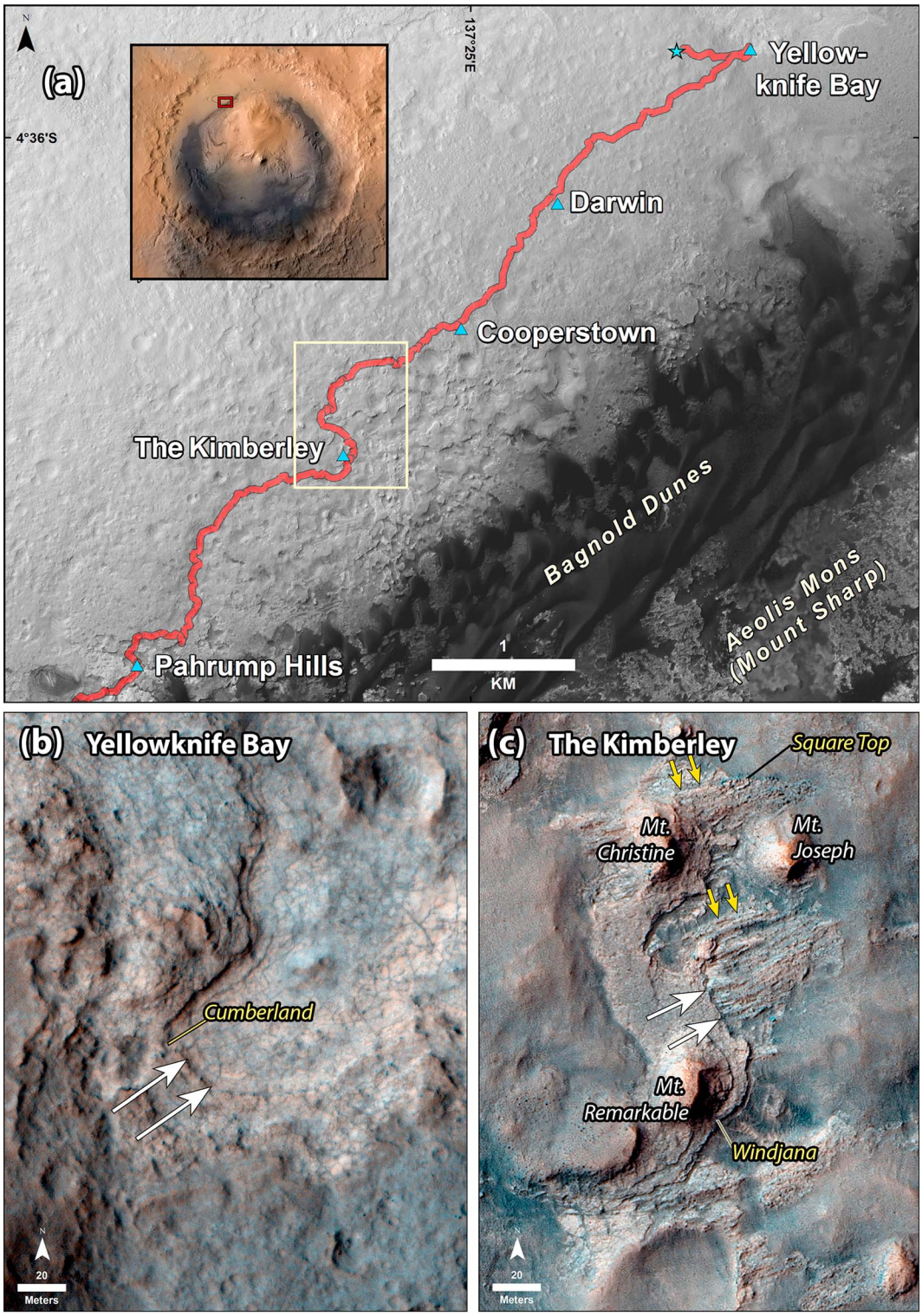

Figure 1. (a) Context map showing location of the Kimberley and other waypoints along Curiosity's traverse to Mount Sharp. The yellow box indicates sols 535–634 (Figure 2). The inset shows the traverse location (red box) within the 154 km diameter Gale crater on the plains to the northwest of Mount Sharp. (b) Detail of Yellowknife Bay shown in HiRISE color. (c) Detail of the Kimberley region shown in HiRISE color. Large white arrows in Figures 1b and 1c indicate scarps at the same orientation (~152°) at both sites. Small yellow arrows in Figure 1c indicate prominent striations in the Square_Top member of the Kimberley formation (see text for details).

Table 1. Summary of Facies Mapped at the Kimberley From Orbital HiRISE Observations [e.g., *Grotzinger et al*., 2015; *Stack et al*., 2016] and Ground-Based Curiosity Observations [e.g., *Le Deit et al*., 2016]

Orbital Facies Name	Description From Orbital Observations[a,b]	Member Name Within the Kimberley Formation[c]	Description From Curiosity Observations[c]
Rugged unit (RT)	Relatively high-albedo outcrops with topographic variability, meter to decameter scale surface roughness, and characterized by erosion-resistant scarps	Beagle	Boulders of sandstone of unknown grain size located at the foot of Mount Remarkable, likely corresponding to erosional remnants of a unit stratigraphically above the Mount Remarkable member
		Mount Remarkable	Structureless, butte-forming unit of unknown grain size
		Dillinger	Decimeter scale cross bedded to fine to very fine sandstone, crosscut by erosionally resistant fracture fills
Orbital striated outcrops (OSO)[a]; striated unit (SR)[b]	Relatively high-albedo outcrops with bluer hues in HiRISE IRB false color and prominent northeast-southwest trending lineations that occur at approximately even meter-scale spacing	Square_Top	South dipping, decimeter thick bedsets of a very coarse sandstone that is mostly planar laminated and interbedded with thinner sandstone
Hummocky Plains (HP)	Relatively low-albedo surfaces with low roughness, uniform tone, and decameter scale topographic hummocks	Liga	Poorly sorted, planar-bedded, granule conglomerate and forms centimeter-scale beds
		Point_Coulomb	Weakly stratified conglomerate with poorly rounded pebbles

[a] *Grotzinger et al*. [2015].
[b] *Stack et al*. [2016].
[c] *Le Deit et al*. [2016].

Mons, and Aeolis Palus have been adopted by the International Astronomical Union. Mount Sharp is an informal name for Aeolis Mons recognizing geologist Robert P. Sharp, and Bradbury Rise is an informal name for the topographic high on Aeolis Palus between Yellowknife Bay and lower Mount Sharp (which includes the rover's landing site, informally named Bradbury Landing after author Ray Bradbury) [*Vasavada et al*., 2014].

2.2. Goals for the Kimberley Waypoint Campaign

A major goal of Curiosity's investigation at the Kimberley was to document the stratigraphy and sedimentology with remote sensing (Mast Cameras (Mastcam) and Chemical Camera (ChemCam)) and contact science (Alpha-Particle X-ray Spectrometer (APXS) and Mars Hand Lens Imager (MAHLI)) observations to determine depositional environments, stratigraphic relationships, diagenesis, and erosional history. In particular, determining the origin of the enigmatic OSO and understanding its connection to other Aeolis Palus strata was a high priority. Another key goal was to identify the sedimentary facies with the highest probability for preserving organic molecules and to drill a sample to deliver to Curiosity's analytical instruments (Chemistry and Mineralogy (CheMin) and Sample Analysis at Mars (SAM)). A drill target was sought in a fine-grained sedimentary unit that might have been deposited in a habitable environment and also was at the base of a retreating scarp indicating recent exposure from beneath several meters of overburden. The site also needed to meet the engineering criteria for drilling, which included a rover placement with all six wheels on a solid surface with no loose rocks, a rover tilt $<7°$, a rover geometry with respect to local topography that would allow for good illumination conditions within the workspace in front of the rover, and a clear line of sight to the orbital spacecraft used for communication.

From the perspective of mission operations, an additional goal was to execute the drilling and sampling activities as efficiently as possible in a constrained number of sols, making use of orbital imagery, mapping, and strategic planning to guide the selection of a drill target. Previously, Curiosity had collected only two drill samples—John Klein and Cumberland—adjacent targets in the Sheepbed mudstone in Yellowknife Bay; the Kimberley would be the first drill campaign acquired "on the road," and the only planned drill location before reaching lower Mount Sharp. Therefore, the Kimberley campaign was treated as a "dress rehearsal" for efficient sampling and characterization of habitability at Mount Sharp. Key observations to be made by each instrument at the Kimberley were prioritized by the science team, in discussions led by the campaign

Table 2. Science Observations That Were Strategically Preapproved and Prioritized by the MSL Science Team Prior to Arrival at the Kimberley

Category	Instrument	Observation
Regional geology characterization	Mastcam stereo	Imaging of striated unit and cliffs north of the Kimberley
	Mastcam stereo	Imaging of the Kimberley through the Mount Joseph and Mount Christine buttes
	Mastcam stereo	Context imaging from the eastern edge of the Kimberley
	Mastcam stereo	Imaging to identify locations for contact science and drilling
	Mastcam left (M34)	360 degree mosaic from drill location
	Mastcam right (M100)	Stratigraphic contacts within the Kimberley
	Mastcam right (M100)	Mosaics looking east from drill location
Unit characterization	Mastcam right (M100)	Imaging of grain size and textures of each unit
	ChemCam	>5 Laser-Induced Breakdown Spectroscopy (LIBS) and Remote Micro-Imager (RMI) observations of each unit
	APXS	Single integration or 2 × 2 raster on each unit
	MAHLI	Imaging of grain size and textures of each unit
	DAN	Active observations of each unit documented with Navcam or Mastcam imaging of DAN field of view
	Mastcam stereo	Imaging of striated beds for dip calculations
Predrilling observations at drill site	Mastcam stereo	Imaging of the workspace
	APXS	>1 h integration on the prebrushed and postbrushed drill target
	MAHLI	Imaging of the prebrushed and postbrushed drill target
	ChemCam	3 × 3 LIBS and RMI raster of the prebrushed and postbrushed drill target
	MAHLI	Self-portrait
Drill hole and tailings characterization	APXS	2 × 2 raster of tailings pile as soon as possible after drilling completed
	APXS	2 × 2 raster of dumped sample pile
	ChemCam	1 × 10 LIBS and passive raster of drill tailings as soon as possible after drilling completed
	ChemCam	1 × 10 LIBS and RMI inside drill hole
	ChemCam	Repeated analysis of tailings and drill hole as opportunities allow
	Mastcam	Multispectral imaging of drill hole and tailings
	MAHLI	Imaging of drill hole and walls
	MAHLI	Imaging of drill holes to use in self-portrait
Sample acceptance and analysis	SAM	Preconditioning and blank cup analysis
	SAM	Preconditioning and Evolved Gas Analysis (EGA), Gas Chromatograph Mass Spectrometer (GCMS) and Tunable Laser Spectrometer (TLS) analyses of solid sample
	CheMin	Solid sample analysis (1–2 cells)
Opportunistic observations	Mastcam and Navcam	Photometry observations from drill location

lead and long-term planners [*Vasavada et al.*, 2014], prior to arrival at the waypoint (Table 2). These preapproved observations were used to guide the tactical planning process during the campaign, but additional science observations were added to each sol's plan opportunistically as time, power, data volume, and other planning constraints allowed.

2.3. Approach to the Kimberley Waypoint, Sols 535–570

On the approach to the Kimberley, bedrock exposures became more frequent in a set of shallow valleys, providing the first opportunities to observe the OSO and other units exposed at the Kimberley. During this approach, the team established a goal of commanding a drive on every possible planning cycle. To

Table 3. Summary of Major Activities During the Kimberley Campaign, Sols 535–634[a]

Sol	Drive (m)	Comment
535	7.0	Drive over Dingo Gap
536	0.0	Science runout
537	0.0	In situ observations on the other side of Dingo Gap
538	4.1	Drive into Moonlight Valley
539	0.0	Imaging of the valley walls
540	73.1	Imaging of the valley walls and drive further into Moonlight Valley
541	0.0	360° imaging
542	22.8	Imaging of outcrops in the valley and drive through Moonlight Valley
543	0.0	Atmospheric monitoring
544	0.0	Wheel imaging and remote science
545	47.0	Drive through Moonlight Valley
546	1.2	Wheel imaging; drive-only sol
547	100.3	Drive toward Junda outcrop; drive-only sol
548	100.1	Imaging of Junda outcrop; Drive through Moonlight Valley; drive-only sol
549	7.0	Drive toward Bungle Bungle target; drive-only sol
550	15.9	In situ observations of JumJum Target
551	0.0	Imaging at an overlook into the Kylie region; drive-only sol
552	79.2	Drive downhill toward Kylie; drive-only sol
553	55.2	Drive toward Kylie and imaging of the valley walls
554	1.2	Imaging of outcrops at Kylie
555	46.7	Imaging of valley walls, drive past Kylie
556	0.0	SAM experiment
557	0.0	SAM experiment
558	0.0	In situ observations of soil
559	57.2	Drive toward the Kimberley; wheel imaging
560	26.3	Contact science
561	30.5	Drive toward the Kimberley
562	1.3	Wheel imaging
563	20.2	Drive south toward Kimberley
564	41.9	Contact science
565	33.2	Drive south toward Kimberley; drive-only sol
566	1.4	Wheel imaging
567	0.0	Remote sensing
568	68.3	Drive south toward Kimberley; drive-only sol
569	102.9	Drive past Jurgurra striated outcrop; drive-only sol
570	0.0	Science runout
571	0.0	Imaging of nearby cliffs
572	89.4	Drive toward Kimberley
573	0.0	Untargeted science
574	38.1	Arrive at the north side of Kimberley
575	0.0	Drive failed due to fault
576	0.0	Clean sampling handling instruments
577	0.0	Fault recovery
578	0.0	Remote sensing at Square_Top
579	0.0	Drive failed due to fault
580	0.0	Imaging of the Kimberley
581	2.9	Bump to Square_Top
582	0.0	Mastcam imaging of the Kimberley
583	0.0	Contact science
584	0.0	Contact science and remote sensing
585	0.0	Contact science
586	1.6	Bump backward
587	22.3	Wheel imaging; leave Square_Top and drive east
588	45.6	Drive to east side of Kimberley at Mount Joseph
589	30.0	Mastcam imaging of the Kimberley; drive south
590	0.0	Mastcam imaging of the Kimberley
591	0.0	Contact science of soil target
592	0.0	Remote ssensing

Table 3. (continued)

Sol	Drive (m)	Comment
593	31.3	Drive along edge of clinoform sandstones and document with Mastcam
594	0.0	Remote sensing
595	55.9	Drive along edge of clinoform sandstones and document with Mastcam
596	0.0	Failed uplink; science runout
597	27.5	Drive to southwestern edge of clinoform sandstones for contact science
598	0.0	High-gain antenna (HGA) telecom anomaly
599	0.0	Science runout
600	0.0	Science runout
601	0.0	Remote sensing and contact science at Liga target
602	0.0	Mastcam imaging of the Kimberley
603	50.7	Decision to drive to SE side of Mount Remarkable for drilling
604	0.0	Drill reconnaissance imaging
605	0.0	Drill reconnaissance imaging
606	19.1	Drive toward drill target
607	0.0	Untargeted science
608	0.0	Remote sensing of candidate drill targets
609	4.8	Bump to Windjana drill target
610	0.0	Remote sensing
611	0.0	CHIMRA vibe; slip check; remote sensing of drill target vicinity
612	0.0	Contact science at Windjana drill target
613	0.0	MAHLI self-portrait
614	0.0	Remote sensing
615	0.0	Windjana minidrill
616	0.0	Recover from MAHLI fault; science runout
617	0.0	Remote sensing
618	0.0	Remote sensing
619	0.0	Remote sensing
620	0.0	Remote sensing
621	0.0	Windjana full drill
622	0.0	Contact science
623	0.0	CheMin analysis
624	0.0	SAM EGA of Windjana
625	0.0	CheMin analysis
626	0.0	Remote sensing
627	0.0	Contact science at Windjana drill hole
628	0.0	Remote sensing and nighttime MAHLI
629	0.0	Contact science at Stephen
630	24.5	Bump back from the drill site; CheMin analysis of Windjana
631	26.6	Imaging of clinoform sandstones; drive away from the Kimberley
632	0.0	Remote sensing
633	0.0	Contact science
634	68.7	Depart the Kimberley

[a]Drive distances indicate the total path length as scaled by visual odometry (the total mission odometry at the start of the campaign on sol 535 was 4918.0 m).

accommodate this schedule, several planning sols were designated as "drive-only sols," with minimal staffing from the science team and instrument observations mostly focused on documenting the traverse with Navcam, Mastcam, MAHLI (from its stowed position), and MARDI. During these sols, Mastcam mosaics were typically the only targeted observations added to support the rover's geologic investigation. When not in the "drive-only" cadence, regular documentation activities were performed with the ChemCam and Dynamic Albedo of Neutrons (DAN) instruments to provide constraints on elemental chemistry without having to deploy the arm. Brief opportunistic science observations with the arm instruments (APXS and MAHLI) were sometimes possible during the approach period, especially within 3 sol weekend plans. Along the traverse, the rover also acquired systematic images of its wheels using MAHLI, in order to document ongoing damage to the wheels that had been documented since sol ~400 [*Vasavada et al*., 2014]. Details of drive distances and

key activities on each sol of the campaign at the Kimberley are provided in Table 3, and details of geologic observations from each instrument are given in Table S1.

While Curiosity encountered the OSO briefly at the Balmville outcrop on sol 513, the rover's approach was not close enough to interpret the sedimentary structures [*Edgar et al*., 2014]. A short time later, on sol 535 (6 February 2014), Curiosity crossed over a transverse aeolian ridge at Dingo Gap (Figures 2 and 3a) in order to enter a narrow valley. Curiosity acquired several large Mastcam mosaics of the sedimentary section exposed in the valley walls as well as in situ observations of the sandstone outcrop targets Halls and Fitzroy on sol 537. Following the RTR, Curiosity continued through Moonlight Valley and made a close approach to the OSO at the Junda outcrop on sol 547, where it first was observed that the regular striations observed from orbit could be attributed to individual beds in a sandstone facies dipping 10–20° to the south. From this point forward, the OSO is referred to as "clinoform sandstones" where observed on the ground [*Grotzinger et al*., 2015].

Upon leaving Junda, Curiosity approached the pebble conglomerate outcrop Bungle_Bungle, which appeared to lie stratigraphically beneath the clinoform sandstones. Mastcam documented Bungle_Bungle on sol 549, and ChemCam, APXS, and MAHLI observed the nearby Jum_Jum conglomerate on sol 550. From this location, Curiosity acquired its first Mastcam mosaics of the Kylie region, where the OSO, RT, and HP units had been identified in orbital images in the same stratigraphic succession as at the Kimberley. Kylie had previously been considered as an alternate waypoint to the Kimberley, but the science team determined that the stratigraphic contacts at the Kimberley were more clearly exposed, and the outcrops in general were less dust covered. The rover drove toward Kylie on sol 552, and over the subsequent 3 sols captured large Mastcam mosaics of outcrop exposed in the valley walls. These images revealed clinoform sandstones that could not be observed from orbit and a complex interfingering of sandstone and conglomerate facies [*Williams et al*., 2015]. At the rover's closest approach to Kylie on sol 554, the first images of the RT unit overlying the clinoform sandstones were acquired, revealing subhorizontal bedding and the presence of cm scale nodules (Figure 3c).

The traverse curved to the southeast after Kylie to avoid the steep cliffs directly between Kylie and the Kimberley. On sols 560 and 564, Curiosity acquired contact science observations of dark, vuggy float rocks (Secure and Monkey_Yard) that might have been remnants of the formerly more extensive capping unit at the tops of cliffs and mesas in the vicinity. On the final approach to the Kimberley, during a series of drive-only sols, Mastcam acquired mosaics of the strata exposed in cliffs to the north of the Kimberley and at Jurgurra, a large outcrop of clinoform sandstones (Figure 3d).

2.4. Geologic Characterization at the Kimberley, Sols 571–609

Curiosity acquired its first long-range reconnaissance imaging toward the Kimberley on sol 571. The rover arrived at the north side of the Kimberley on sol 574, approaching a prominent rock ridge that had been identified from orbit as clearly exposed and relatively dust free (as indicated by the blue hues in the HiRISE false-color images; Figure 1c). Near the target Square_Top along this ridge, the rover experienced a remote sensing mast fault on sol 575 and an arm fault on sol 578, which kept Curiosity at this location for four additional sols, during which extended imaging of the Kimberley from the north was possible (e.g., Figures 4a and 4b). Following fault recovery and diagnostics, Curiosity bumped forward on sol 581 to perform an extended contact science campaign to characterize the Square_Top strata (Square_Top and Virgin_Hills targets) and the underlying granule conglomerates (Panadus_Yard). After this target, the clinoform sandstone at the Kimberley was named the Square_Top member of the Kimberley formation [*Grotzinger et al*., 2015; *Le Deit et al*., 2016]. These observations from sols 583 to 585 show that the clinoform sandstones are composed of fine sands with dispersed coarser grains (from 0.5 to 3.1 mm in diameter) [*Grotzinger et al*., 2015]. After leaving the Square_Top location, Curiosity traversed east and imaged a pebble conglomerate outcrop named Point_Coulomb. These conglomerates are consistently observed at the base of the stratigraphic section and have been collectively termed the Point_Coulomb member of the Kimberley formation [*Mangold et al*., 2016; *Le Deit et al*., 2016].

On sol 588, the team celebrated the "arrival" at the Kimberley, after rounding the eastern side of the Mount Joseph butte (the team had designated this spot as the "entrance" to the Kimberley outcrops; however, in this paper we designate sol 574's drive to Square_Top as the arrival at the Kimberley, as this was Curiosity's first

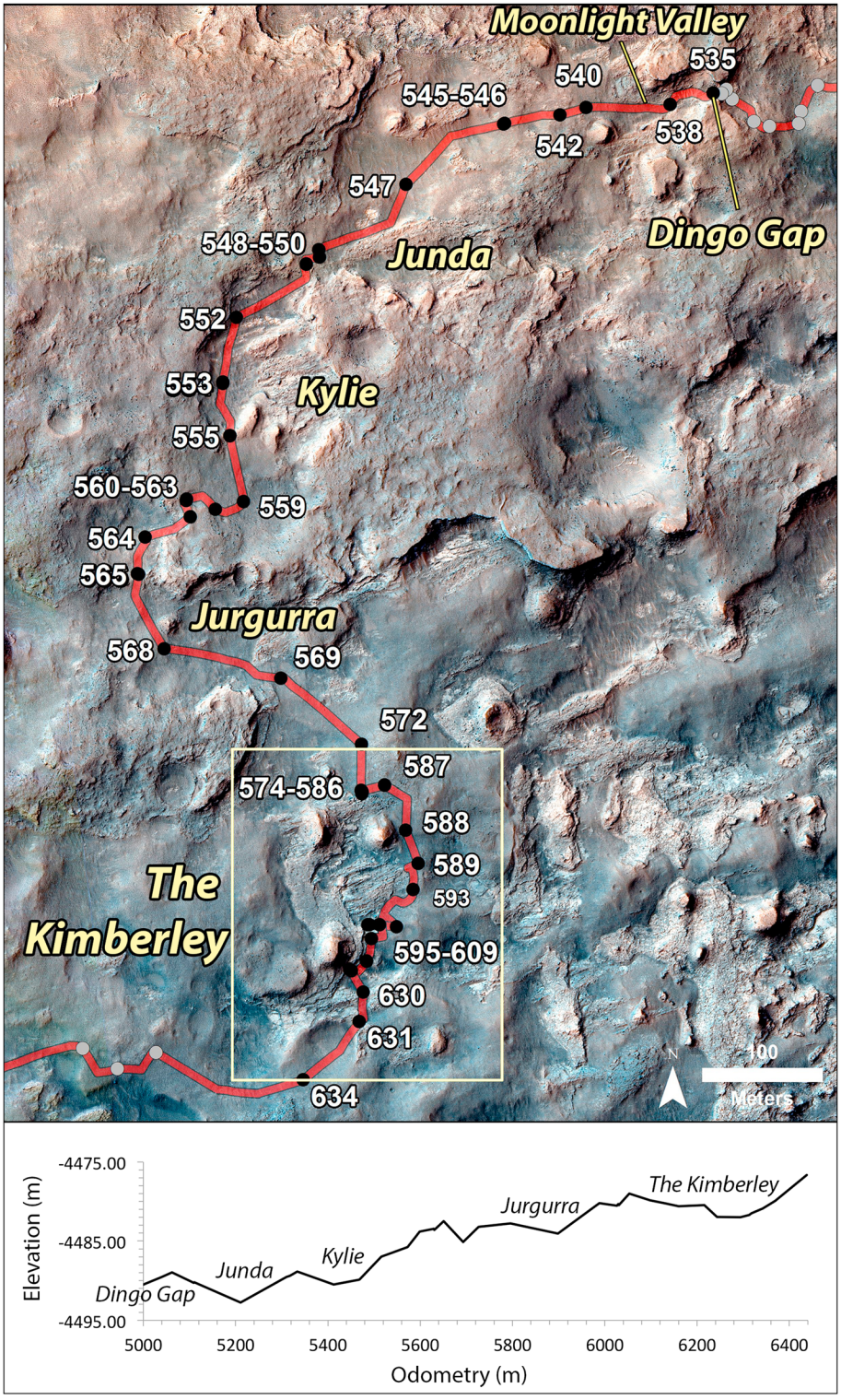

Figure 2. Traverse map for sols 535–634 showing the end-of-drive locations on each sol during the approach to the Kimberley waypoint and during the Kimberley campaign (drive distances provided in Table 3), with locations of key features and outcrops (shown in Figure 3). The yellow box outlines the location of the Kimberley outcrops shown in Figure 1c. The elevation profile during this portion of Curiosity's traverse shows an increasing gain in elevation as the rover drove south.

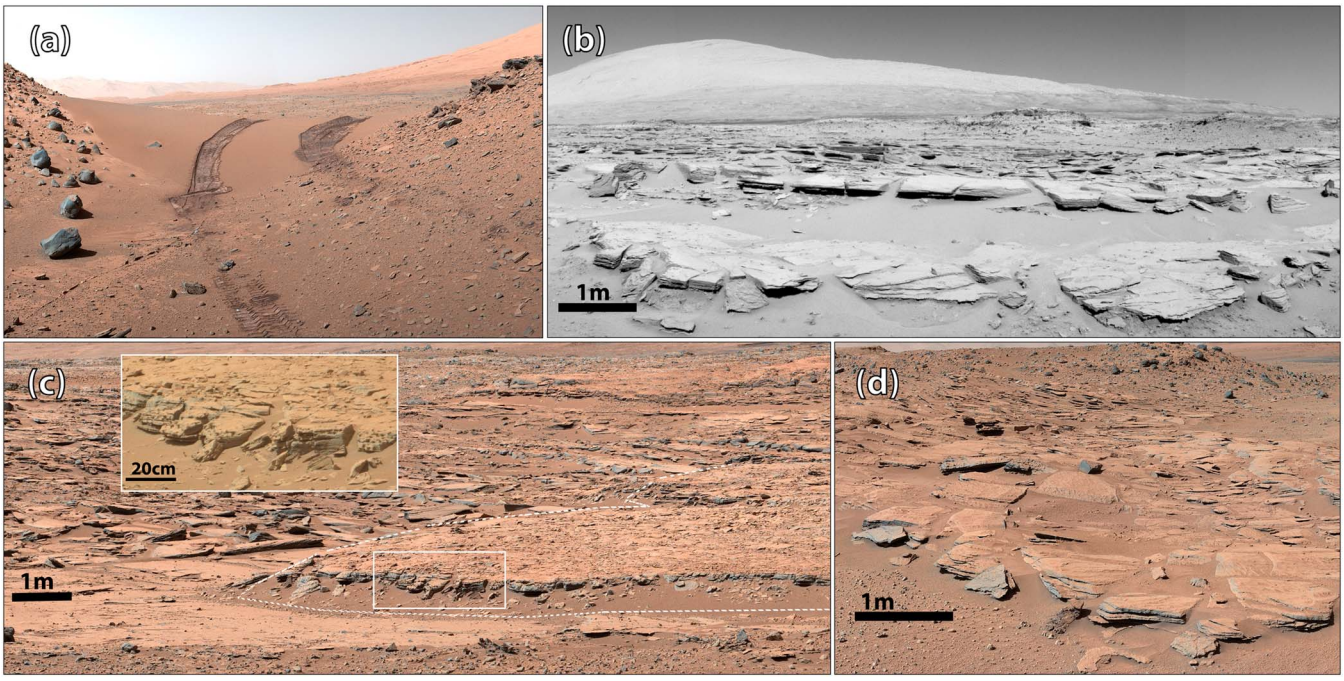

Figure 3. Example mosaics from key locations along the approach of the Kimberley: (a) sol 538 white-balanced Mastcam-34 mosaic (sequence ID mcam02124) from of the Dingo Gap transverse aeolian ridge, with wheel tracks ~3 m apart for scale; (b) sol 548 Navcam mosaic (sequence ID ncam00477) of the Junda outcrop with Mount Sharp in the background; (c) sol 554 white-balanced Mastcam-100 mosaic (sequence ID mcam02246) of sandstone outcrops at Kylie, with the dashed white line indicating the contact seen from orbit between the OSO and RT units (see text for discussion). The inset shows detail of bedding and erosion-resistant nodules in the overlying RT unit; (d) sol 569 white-balanced Mastcam-34 mosaic (sequence ID mcam02310) of the Jurgurra outcrop.

encounter with the rocks of the Kimberley formation). Looking along strike of the striations in the clinoform sandstone, several large Mastcam mosaics were acquired for context. From here, the team selected the southwestern edge of the clinoform sandstones, at the base of the Mount Remarkable butte, as the best location to access the contacts between rock units and select a drill target. On sols 593–595, Curiosity drove southwest along the edge of the clinoform sandstones, systematically acquiring Mastcam stereo images ("multistop" observations in Table 3) to the side of the rover to document variations in texture, grain size, and bedding geometries.

On sol 601, Curiosity examined the unit underlying the clinoform sandstones at the Liga target, where MAHLI observations revealed inclined, interstratified granule- and pebble-rich beds and sandstone beds with poorly sorted, subangular to subrounded grains as large as 4.7 mm in diameter [*Grotzinger et al*., 2015]. This unit, which lies stratigraphically between the Point_Coulomb and Square_Top members, has been termed the Liga Member of the Kimberley formation [*Grotzinger et al*., 2015; *Le Deit et al*., 2016]. From this location, Curiosity also acquired its first close look at the unit overlying the clinoform sandstones, which had been previously glimpsed at Kylie and mapped from orbit as the RT unit. Mastcam mosaics indicated that this unit was thinly bedded, fine-grained, internally laminated, and contained dark-toned, erosionally resistant fracture fills. The apparently structureless material of the overlying butte, Mount Remarkable, was observed to have a small scarp at its base and dark-toned, erosionally resistant boulders on its flanks that are likely remnants of a former more resistant unit that is now eroded from the top of Mount Remarkable. Taken together, these observations suggest that Mount Remarkable may represent a former mesa in its final stages of erosion. The morphologic similarity of the Mount Remarkable scarps to the actively eroding scarp studied previously at Yellowknife Bay [*Farley et al*., 2014] suggests that the underlying outcrops may have been exposed on comparably recent timeline ($<$100 Ma).

On sol 603, the team discussed options for drilling at the Kimberley and decided that the RT unit beneath Mount Remarkable would be the best candidate, given its fine grain size and hypothesized recent exposure. However, the closest RT unit to the rover at this point would have required a two-sol traverse across a stretch of fractured clinoform sandstones in order to position the rover for drilling, which raised concerns about

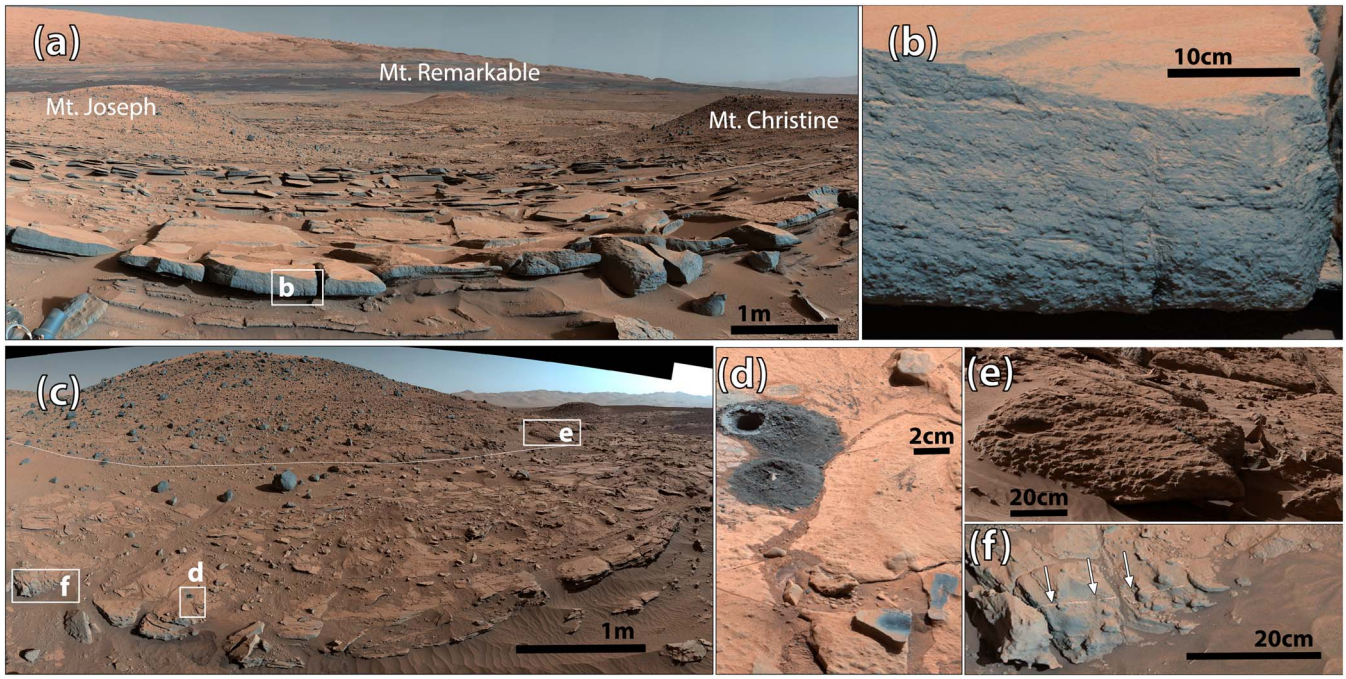

Figure 4. Mastcam mosaics of key outcrop locations during the Kimberley campaign, with examples of sedimentary and diagenetic textures: (a) sol 580 white-balanced Mastcam-34 mosaic (sequence ID mcam02407) of the Kimberley outcrops at Square_Top, with the three Kimberley buttes and Mount Sharp in the background; (b) detail of grains and bedding in the Square_Top sandstone from the sol 576 white-balanced Mastcam-100 mosaic (sequence ID mcam02368); (c) sol 620 white-balanced Mastcam-34 mosaic (sequence ID mcam02652) of the Kimberley outcrops at Windjana, with the white line indicating the contact between the Dillinger and Mount Remarkable members, and dark boulders interpreted to be remnants of the overlying Beagle member; (d) detail of the Windjana drill hole and adjacent high-Mn targets; (e) example of erosion-resistant nodules within the Mount Remarkable member; and (f) example of light-toned, Ca-sulfate fracture-filling vein in the Dillinger member.

ongoing wheel damage [*Vasavada et al*., 2014]. The science team opted instead to traverse ~75 m across smoother terrain to an alternate drilling location beneath the southeastern flank of Mount Remarkable (Figures 1c and 4c). Curiosity made this traverse in two drives on sols 603 and 606, acquiring several Mastcam mosaics for context. On sol 608, ChemCam acquired the first analyses in the vicinity of the drill target, marking the start of an extended campaign to characterize the RT unit. The RT unit has since been termed the Dillinger member of the Kimberley formation after one of the ChemCam targets.

2.5. Activities at the Windjana Drill Site, Sols 610–629

Along an outcrop of the Dillinger member on the southeast side of Mount Remarkable, the target Windjana was selected as having the best geometry for drilling. Predrill contact science observations (the dust-removal tool: DRT, MAHLI, and APXS) were performed on sol 612 to vet the chemistry and texture of the desired drill target, and a self-portrait of Curiosity at the drill site was taken with MAHLI on sol 613 to document the geologic context and the complete sampling activities at a drill site. A 20 mm deep test drill ("mini-drill") was successfully performed on sol 615 to assess the suitability of the target for drilling as well as sample delivery to CheMin and SAM, but a fault with the MAHLI instrument on this sol precluded drilling the full sample until sol 621. Sols 616–620 were used for fault recovery and extensive remote sensing at the drill site, including ChemCam documentation of the Dillinger member, diagenetic fracture-fills, bedrock targets on Mount Remarkable, and out-of-place dark-toned boulders of the Beagle member of the Kimberley formation inferred to represent strata that once capped the top of the Mount Remarkable butte [*Le Deit et al*., 2016]. ChemCam and APXS chemical analyses of all members of the Kimberley formation showed that their overall abundances of K_2O were substantially higher than average Mars crust [*Le Deit et al*., 2016; *Thompson et al*., 2016]; the implications of these results for sediment provenance are discussed in section 4. ChemCam observations of the Dillinger member also revealed high Zn in all targets (up to 8.4 wt % at Yarrada, sol 628), as described in detail by *Lasue et al*. [2016].

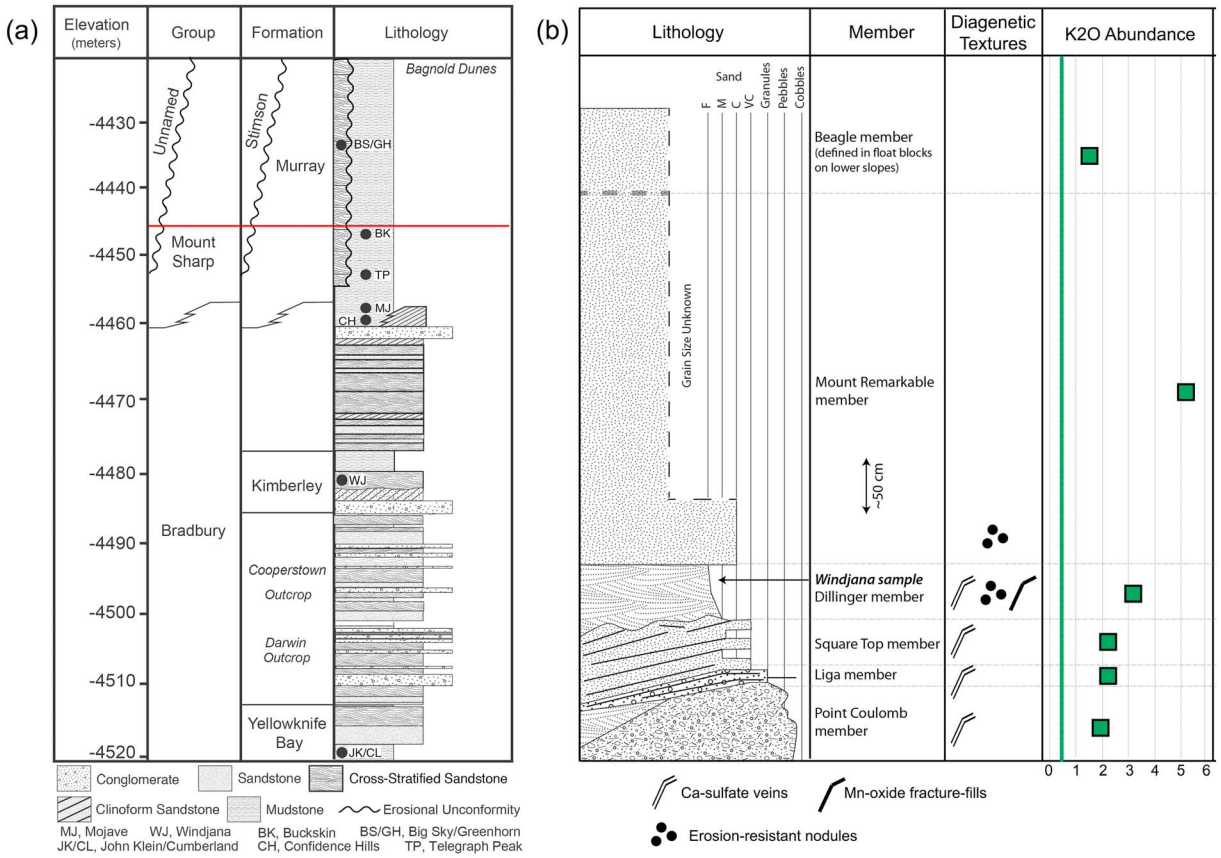

Figure 5. Regional stratigraphic context and details of the Kimberley formation: (a) Stratigraphic column for the sedimentary facies from Yellowknife Bay to the Bagnold Dunes, with the traverse shown in Figure 1a represented below the red line. The contact between the Bradbury group (Aeolis Palus) and the Mount Sharp group (Aeolis Mons) is marked by interfingering of facies [*Grotzinger et al*., 2015]. (b) Stratigraphic column for the Kimberley formation with diagenetic textures indicated, plotted with average K_2O abundances for each member from ChemCam observations [*Le Deit et al*., 2016]. The average Mars crustal K_2O abundance of 0.45% [*Taylor and McLennan*, 2009] is plotted in the green vertical line for comparison.

The 65 mm full drill hole (Figure 4d) produced a sample of powdered rock at Windjana on sol 621 that was delivered to the CheMin instrument for analysis on sol 623. The CheMin X-Ray Diffraction (XRD) pattern constrained the mineralogy of the K-rich sediment component as sanidine and provided little evidence for low-temperature aqueous alteration, as described by *Treiman et al*. [2016]. The Windjana sample was delivered to the SAM instrument for an evolved gas analysis (EGA) experiment on sol 624. The drive away from the Windjana location was initially planned for sol 629, but in response to the first ChemCam and APXS measurements of the fracture-fill target Stephen, which revealed surprisingly high Mn concentrations, revealing apparent Mn oxides [*Lanza et al*., 2016], the departure was delayed to allow for an additional sol of contact science of this target.

2.6. Departure From the Kimberley, Sols 630–634

Curiosity departed from the Kimberley region in three drives on sols 630, 631, and 634. Along the exit route to the south, the rover acquired additional Mastcam mosaics of clinoform sandstone outcrops and ChemCam observations of granule conglomerates of the Liga member. A final set of contact science observations at the target Wift (of the Liga member) was performed on sol 633. Upon leaving the Kimberley, Curiosity retained some drill cuttings of the Windjana sample material cached within the Collection and Handling for Interior Martian Rock Analysis (CHIMRA) in order to permit additional SAM analyses; this allowed for crystallization age and cosmogenic exposure age experiments to be performed later [*Vasconcelos et al*., 2016].

3. Stratigraphy and Depositional Environments at the Kimberley

The outcrops encountered at the Kimberley appear to show a fining-upward succession: pebble conglomerates at the base of the Kimberley formation (Point_Coulomb member), granule conglomerates and

sandstones (Liga member), clinoform sandstones (Square_Top member), fine-grained, low angle and undulatory laminated sandstones (Dillinger member), and massive, butte-forming outcrop (Mount Remarkable member) and dark-toned capping rocks (Beagle member) of unknown grain sizes. This stratigraphy of the Kimberley formation is summarized in Figure 5, and described in detail by *Le Deit et al*. [2016].

The south dipping Square_Top member sandstones have been interpreted as small-scale delta clinoforms [*Grotzinger et al*., 2015]. The presence of large grains (up to 3.1 mm in diameter) observed in MAHLI observations at Square_Top requires transport by water rather than by wind. The underlying conglomerates of the Liga and Point_Coulomb members are also interpreted as being formed by migrating subaqueous bed forms or barforms in a fluvial environment, similar to the interpretation of conglomerates observed early in Curiosity's mission prior Yellowknife Bay [*Williams et al*., 2013]. The rounding of clasts within the conglomerates suggests transport distances of tens of kilometers [*Szabó et al*., 2015], which is consistent with deposition in an alluvial fan environment and transport from Gale crater's northern rim (section 4).

The Dillinger member forms a subhorizontal stratal unit of very fine-grained sandstone or siltstone (with grains at or below the grain size detection limit of MAHLI [*Treiman et al*., 2016]) that is approximately 0.5 m thick and overlies the Square_Top member across a distinct truncation surface [*Grotzinger et al*., 2015]. Analysis of multiple Mastcam mosaics demonstrates that the Dillinger member is characterized by the presence of undulose lamination-forming mounded bed geometries; similar bedset geometries have been described from a number of ancient terrestrial fluvial examples and linked to conditions characterized by abrupt discharge variability [*Gupta et al*., 2014].

Multiple sediment transport directions have been reconstructed from cross-bed dip directions that suggest an ancient fluvial (or possibly mixed fluvial-aeolian) system with a primarily southwesterly flow [*Grotzinger et al*., 2015]. Some observations of sets of cross beds in the Dillinger show a reverse in dip between north and south, and these beds may have been deposited by small aeolian dunes when lake levels were low [*Rubin et al*., 2015], indicating that lake levels would have fluctuated over the period of sediment deposition at the Kimberley, allowing for intermittent periods of subaerial exposure.

Similar conglomerate, clinoform sandstone, and cross-bedded sandstone facies to those of the Kimberley formation have been observed in the valley walls near Dingo Gap [*Edgar et al*., 2014], at Kylie [*Williams et al*., 2015], and in cliff faces immediately north of the Kimberley. The same facies observed at multiple locations across Curiosity's ~1.5 km traverse during the Kimberley campaign, over an elevation gain of ~12 m, do not represent the same stratal units, but rather distinct units that were stacked during fluvial progradation, which is commonly the case in terrestrial fluvial-lacustrine deposits [*Grotzinger et al*., 2015]. Where observed in cross section in cliffs and valley walls, the clinoform sandstones are 1 to 4 m thick, suggesting water depths shallower than a few tens of meters [*Grotzinger et al*., 2015].

The interpretation of the clinoform sandstones as having been primarily transported from the north and deposited in small deltas implies a transition to lacustrine facies within the basin was likely to occur farther to the south. Curiosity tested this hypothesis along its continued traverse southwest at Pahrump Hills, where thinly laminated lacustrine mudstones were indeed encountered within the Murray formation [*Grotzinger et al*., 2015], further validating a fluvio-lacustrine interpretation for the depositional environment at the Kimberley.

The geochemistry of the Kimberley formation, as revealed by analyses of APXS [*Thompson et al*., 2016] and ChemCam [*Le Deit et al*., 2016] observations, shows that little alteration of the primary igneous minerals in the sediments occurred during deposition. The CheMin analyses described by *Treiman et al*. [2016] show that the Windjana drill sample contains only igneous minerals and their low-temperature alteration products: sanidine (21% weight, ~Or_{95}); augite (20%); magnetite (12%); pigeonite; olivine; plagioclase; amorphous and smectitic material (~25%); and percent levels of others including ilmenite, fluorapatite, and bassanite. From mass balance on the APXS analysis of the Windjana drill tailings, the amorphous component is Fe rich with almost no other cations (e.g., ferrihydrite). There are no detectable concentrations of minerals observed by CheMin that would suggest metamorphism or hydrothermal alteration, and no minerals that are characteristic of most chemical sediments (e.g., carbonates or silica) except iron oxyhydroxides [*Treiman et al*., 2016]. The Dillinger member sandstone, therefore, is likely cemented by magnetite and ferrihydrite. The low-albedo and shallow blue-to-red spectral slope of the Windjana drill tailings, as observed in quantitative visible/near-infrared reflectance spectra from ChemCam passive and Mastcam multispectral observations, are consistent with the presence of these mineral phases [*Johnson et al*., 2016; *Wellington et al*., 2016].

Observations from the DAN instrument on the lower members of the Kimberley formation (Dillinger, Square_Top, Liga and Point_Coulomb members) confirm that there is very little water-equivalent hydrogen in these outcrops, consistent with a lack of hydrated minerals from aqueous alteration. *Litvak et al.* [2016] describe how DAN observations at the Kimberley are best described by a two-layer model with ~2.3% water in the top 15 cm and 1.4% water in the bottom layer. This inferred hydration in the upper layer is consistent with estimates from SAM EGA analyses of the Windjana sample [*Litvak et al.*, 2016]. DAN also measured variations in neutron-absorbing elements throughout the stratigraphy of the Kimberley formation, observing a general decrease in a modeled parameter called the chlorine-equivalent concentration with increasing stratigraphic position, consistent with measurements of Cl made by APXS at the Kimberley [*Litvak et al.*, 2016].

Collectively, these data suggest that weathering, transport, and diagenesis of the sediment did not occur in a warm and wet environment, but under low temperatures and low water-to-rock ratios and/or low oxygen fugacity. *Thompson et al.* [2016] argue further that water-to-rock ratios may have been too low to explain the entire deposition of the Kimberley formation by fluvio-deltaic processes, and they suggest some sediment may have been transported into Gale crater via glacial/periglacial processes in a cold, icy environment [e.g., *Le Deit et al.*, 2013; *Fairén et al.*, 2014; *Oehler et al.*, 2016]. While some of the conglomerates observed at the Kimberley (targets Bungle_Bungle and Jum_Jum) show particle characteristics (sizes, shapes, fabrics, compositions, and sorting) consistent of supraglacial till, no clear sedimentological evidence for deposition in a glacial environment (e.g., dropstones, frost wedges, or tills) has been observed at the Kimberley or elsewhere along the rover traverse.

4. Sediment Provenance

The interpretation of the south dipping sandstones at the Kimberley as having been deposited in small, southward prograding deltas requires that sediment was transported from higher elevations in the north, likely from the north rim and walls of Gale crater. The sedimentary rocks that Curiosity had previously examined at Yellowknife Bay and on Bradbury Rise were also sourced from the north crater rim [e.g., *Grotzinger et al.*, 2014; *McLennan et al.*, 2014; *Palucis et al.*, 2014], but the composition of rocks at the Kimberley suggests differences in provenance. As described by *Mangold et al.* [2016], the conglomerate outcrops observed by ChemCam on Bradbury rise (prior to sol 540) have a felsic alkali-rich composition (with a $Na_2O/K_2O > 5$), whereas those observed during the Kimberley campaign have an alkali-rich potassic composition with $Na_2O/K_2O < 2$. ChemCam observations of the other members of the Kimberley formation are described in detail by *Le Deit et al.* [2016] and suggest an overall mean K_2O abundance that is significantly greater than had been previously observed by Curiosity, and more than 5 times higher than that of the average Martian crustal value of 0.45 wt % [*Taylor and McLennan*, 2009]. This K_2O abundance generally increases upward through the stratigraphic section or is more enriched in finer-grained sediments (Figure 5) [*Le Deit et al.*, 2016; *Thompson et al.*, 2016]. APXS observations show that high potassium content is associated with elevated abundances of iron, magnesium, manganese, and zinc and diminished abundances of sodium, aluminum and silicon, relative to average Mars [*Thompson et al.*, 2016].

CheMin analyses show that the abundant potassium in the Windjana sample is contained nearly entirely in the K-rich feldspar sanidine [*Treiman et al.*, 2016]. Although alkali-rich igneous rocks have been previously encountered in several places in Gale crater [*Sautter et al.*, 2015] and are present in the Martian meteorite NWA 7034 [e.g., *Santos et al.*, 2015; *Wittmann et al.*, 2015], felsic rocks on Mars appear so far to be rare [e.g., *Sautter et al.*, 2016]. Alkali feldspars are notably difficult to observe in the infrared bands, essentially only appearing when Fe substitutes for Ca [e.g., *Serventi et al.*, 2013]. To date, no alkali feldspars have been confirmed from orbit; the limited identification of feldspars made by the orbital Compact Reconnaissance Imaging Spectrometer for Mars instrument is most consistent with anorthitic plagioclase [*Carter and Poulet*, 2013; *Wray et al.*, 2013], and no alkali feldspars have been uniquely detected from Mars Global Surveyor Thermal Emission Spectrometer observations [e.g., *Bandfield*, 2002; *Rogers and Hamilton*, 2015; *Rogers and Nekvasil*, 2015]. Therefore, CheMin's analysis at Windjana is the first mineralogical detection of an alkali feldspar on Mars and is an opportunity to gain new insights into the planet's magmatic evolution. *Treiman et al.* [2016] argue that the alkaline magmas could have been low volume partial melts of metasomatized mantle, in which case Mars would have had a differentiating and (probably) fluid-bearing mantle before the melting, eruption, and crystallization of igneous rocks on Gale crater's north rim, which

has been dated to 4.21 ± 0.35 Ga [*Farley et al*., 2014]. Few alkaline igneous rocks of this age are known on Earth, suggesting that the Martian mantle had differentiated far earlier than the Earth, which is consistent with thermochemical models of Mars' early mantle [*Baratoux et al*., 2013; *Filiberto and Dasgupta*, 2015].

The chemistry at the Kimberley contained additional surprises based on ChemCam data, including the detection of fluorine in a number of observations [*Forni et al*., 2015a]. A large fraction of these observations come from the Kimberley, where F abundances were observed in the range of 0.2 to 0.8 wt %, and were correlated with K, Al, Si, and Mg, in decreasing order [*Forni et al*., 2015b]. Investigation of the chemical trends of the targets with the highest potassium yielded predictions of phlogopite [*Treiman and Medard*, 2016], consistent with the fluorine observations.

Unfortunately, attempts to refine the crystallization ages of the Kimberley sediments using SAM data from Windjana were unsuccessful, as described by *Vasconcelos et al*. [2016]. An aliquot heated to ~915°C yielded a K-Ar age of 627 ± 50 Ma, and reheating the same aliquot to verify complete extraction yielded no additional Ar. A second aliquot heated in the same way yielded a much higher K-Ar age of 1710 ± 110 Ma; these discordant data are most readily understood as arising from incomplete Ar extraction from a rock with a K-Ar age older than 1710 Ma. Most likely, however, the protoliths for the Kimberley sedimentary rocks have similar crystallization ages as those elsewhere on the north rim of Gale crater, which are Noachian (~4.2 Ga) [*Farley et al*., 2014; *Le Deit et al*., 2013; *Thomson et al*., 2011].

In addition to the potassium-rich alkali feldspar source, ChemCam observations suggest at least two additional bedrock petroliths for the Kimberley sediments: (1) a component is rich in mafic minerals, with little feldspar (similar to a shergottite); and (2) a component is richer in plagioclase and in Na_2O, likely to be basaltic [*Treiman et al*., 2016]. The presence of significant percentages of easily weathered primary igneous minerals such as olivine, pyroxene, and pyrrhotite, and the absence of any hydrous silicate minerals indicates that significant water-based alteration did not occur at the sediment source or during cementation. Instead, the mixtures of distinct igneous petroliths are the likely origin of observed chemical variations through the stratigraphic section [*Le Deit et al*., 2016; *Mangold et al*., 2016; *Thompson et al*., 2016; *Treiman et al*., 2016]. Physical sorting of fine potassium feldspar grains into the finest-grained sediments may have also played a role in the enrichment in K_2O in the Kimberley formation, although this still requires a distinct igneous source of potassium feldspar since other mineral sorting trends in the Bradbury group segregate coarse feldspar grains from fine-grained mafic minerals [*Le Deit et al*., 2016; *Mangold et al*., 2016; *Siebach et al*., 2015; *Thompson et al*., 2016]. The presence of sediment from multiple igneous sources, in concert with Curiosity's previous identifications of other igneous materials (e.g., the mugearite rock Jake Matijevic [*Sautter et al*., 2014; *Stolper et al*., 2013]), implies that the northern rim of Gale crater exposes a diverse igneous complex, at least as diverse as those found in similar-age provinces on Earth [*Mangold et al*., 2016; *Treiman et al*., 2016].

Elevated trace element concentrations in the Dillinger unit relative to surrounding units imply a mechanism for concentrating these elements, whether by integration of particles from a concentrated source rock (sediment provenance) or by later fluid flow through the Kimberley units (diagenesis). *Thompson et al*. [2016] describe elevated Zn, Ge, and Cu detected by APXS in the Windjana drill tailings, and *Lasue et al*. [2016] describe the confirmation by ChemCam of elevated Zn (averaging about 0.2 wt % but present up to 8.4 wt %) in up to 20% of targets within the Dillinger member, independent of rock texture. *Lasue et al*. [2016] propose that the Zn could be in the form of Zn-oxides; however, *Lanza et al*. [2016] show that Zn is not correlated with the occurrences of Mn-oxides observed at the Kimberley (section 5). A lack of sulfur suggests the Zn phase is not sphalerite, and correlation with Na_2O suggests it could be in an amorphous clay such as sauconite [*Lasue et al*., 2016]. *Lasue et al*. [2016] and *Thompson et al*. [2016] suggest that localized hydrothermal alteration in the source rocks at the northern rim of Gale could create trace-metal-enriched sediment that then contributed to the Dillinger formation, although no hydrothermal minerals are present at the detection limit of CheMin in the analysis of Windjana. *Thompson et al*. [2016] and *Lanza et al*. [2016] discuss very significant trace-metal enrichment along diagenetic fractures within the Dillinger sandstone, so it is also possible that the trace metals were concentrated in the Dillinger during cementation and later diagenetic processes.

5. Diagenetic Alteration

Although the Windjana sample likely experienced only limited chemical alteration or weathering, given its abundance of easily altered minerals like plagioclase, olivine, pyrrhotite, and sanidine [*Treiman et al*., 2016],

there is evidence elsewhere in the Dillinger member and other rock units at the Kimberley for diagenetic alteration. Light-toned veins have been observed in the Dillinger, Square_Top and Liga, and members of the Kimberley formation [*Grotzinger et al*., 2015] and are observed near Windjana (Figure 4f). Similar light-toned veins were observed in Yellowknife Bay and near the Kimberley and beyond [e.g., *Kronyak et al*., 2015; *Nachon et al*., 2014]. The Windjana sample contains small amounts (near detection limits) of the calcium sulfates bassanite and anhydrite, which are likely related to the Ca-sulfate veins in the Windjana area, although no veins are observed within MAHLI observations of the drill hole walls.

In addition to the light-toned veins, the Dillinger member also contains dark-toned, erosionally resistant fracture fills with high-Mn abundances ($>$25 wt % MnO), as observed at the ChemCam targets Stephen, Neil, and Mondooma (e.g., Figure 4d). The Mn in these targets correlates with trace metal abundances but not with other elements such as C, Cl, and S, which suggests that these deposits are Mn oxides rather than other salts or evaporites [*Lanza et al*., 2016]. This indicates that after the strata were deposited, lithified, and fractured, highly oxidizing fluids moved through the fractures and precipitated the Mn-oxide veins. Based on the strong association between Mn-oxide deposition and changing atmospheric O_2 levels on Earth, *Lanza et al*. [2016] argue that the presence of these Mn phases at the Kimberley means that there were higher concentrations of molecular oxygen within the atmosphere and some groundwaters of Mars in the past. No cross-cutting relationships have been observed between the light-toned Ca-sulfate veins and the Mn-oxide materials, and thus we are unable to place constraints on the relative timing of the two fracture-filling diagenetic events. However, it is clear that at least two distinct fluid-flow events with different aqueous chemistries had occurred within the Dillinger member.

At some exposures of the Dillinger and Mount Remarkable members at the Kimberley (Figure 4f), and in similar facies at Kylie (Figure 3c inset), Mastcam images of the outcrops show spherical protrusions that are relatively uniform in size and dispersed with varying spatial distributions [*Williams et al*., 2015]. These nodules appear similar to those seen previously in Yellowknife Bay, although they are significantly larger (cm scale at the Kimberley, as opposed to $<$ 5 mm in the Sheepbed mudstone). The Sheepbed nodules have a higher Fe content than the surrounding outcrops and have been interpreted as concretions formed during early diagenesis [*Stack et al*., 2014], possibly by the alteration of olivine and/or glass [*Schieber et al*., 2016]. Unfortunately, compositional data for the nodules at the Kimberley could not be acquired as the rover did not come within the ~5 m distance to these concretions required for obtaining high-quality ChemCam data, and a definitive origin for these features cannot be determined.

6. Landscape Evolution

The interpretation of the Kimberley formation as having formed at the margins of a rising lake implies that the downhill direction must have been to the south during the time of sediment deposition. The current topography slopes to the north, in the direction away from Mount Sharp; therefore, there was once a basin where there is now a mountain, and deposition of the Kimberley formation would have to predate the deposition of the bulk of Mount Sharp. In this model, a substantial amount of erosion and removal of material from Gale crater must have subsequently occurred in order to explain the modern topography. Although the exact process by which this occurred is unknown, the mechanical breakdown of crater-filling bedrock by aeolian abrasion and removal of sediment by winds has been previously suggested for Gale crater [e.g., *Malin and Edgett*, 2000] and other craters with sedimentary mounds [*Day et al*., 2016; *Bennett and Bell*, 2016]. Extensive evidence for aeolian abrasion has been observed along Curiosity's traverse in the form of ventifacts [*Bridges et al*., 2014] and actively retreating scarps [*Farley et al*., 2014], and the rover has encountered the full spectrum of progressive surface denudation from fractured bedrock, to retreating bedrock-capped mesas, to remnant hills capped by bedrock rubble, and to desert pavement plains [*Day and Kocurek*, 2016]. The geomorphology at the Kimberley suggests a landscape that has undergone—or is still undergoing—this process of denudation, with three buttes of the Mount Remarkable member covered with boulders of the Beagle member that are interpreted to be the remnants of former mesa-capping bedrock. Crater statistics of Aeolis Palus and the base of Mount Sharp indicate that the exhumation and exposure of most of the Gale crater floor had occurred by ~3.3 billion to 3.1 billion years ago [*Palucis et al*., 2014; *Grant et al*., 2014]. Therefore, the landscape at the Kimberley may have acquired most of its present expression by the middle Hesperian Period, with a long epoch of slow aeolian erosion continuing to the present.

At the Windjana drill site, Curiosity was able to test hypotheses about ongoing aeolian abrasion and deflation leading to the recent exposure of the lower members of the Kimberley formation. Specifically, as described by *Vasconcelos et al.* [2016], the error-weighted mean surface exposure age from ^{3}He and ^{21}Ne in SAM analyses of the Windjana sample is 46 ± 16 Ma, which is a minimum exposure age given the possibility of incomplete extraction (however, the concordance between the ^{3}He (30 ± 27 Ma) and ^{21}Ne (54 ± 19 Ma) ages provides no evidence for underextraction). The exposure of the Windjana target from beneath the Mount Remarkable member may have occurred via scarp retreat at ~46 Ma, via vertical erosion occurring at a mean rate of ~1.5 cm Ma^{-1}, or some combination of erosional processes [*Vasconcelos et al.*, 2016]. This inferred erosion rate at the Kimberley is similar to that reported previously for the Sheepbed-Gillespie scarp at Yellowknife Bay [*Farley et al.*, 2014], implying that rates of erosion by aeolian abrasion may be similar across Aeolis Palus.

7. Conclusions and Remaining Questions

The results from Curiosity's campaign at the Kimberley, summarized here and in this special section of *Journal of Geophysical Research-Planets*, suggest the following sequence of events for the geologic evolution of Gale crater.

1. Potassium feldspars formed in alkaline igneous rocks, emplaced on what is now the north rim and walls of Gale crater, suggesting that the Martian mantle had differentiated significantly by the late Noachian, far earlier than similar differentiation occurred on Earth.
2. Sediments eroded from this alkali feldspar protolith and other diverse igneous sources were transported to the floor of Gale crater from the northern rim and deposited at the Kimberley in a prograding, fluvio-deltaic system during the late Noachian to early Hesperian, prior to the existence of most of Mount Sharp.
3. Lake levels fluctuated during the period of deposition, and the Kimberley was at times covered by up to tens of meters of water and at times dry.
4. Sediment deposition likely took place under cold conditions with relatively low water-to-rock ratios.
5. After deposition, the rocks at the Kimberley were buried and underwent multiple episodes of diagenetic alteration with different aqueous chemistries and redox conditions to deposit Ca-sulfate veins, Mn-oxide fracture-fills, and erosion-resistant nodules.
6. Starting in the middle Hesperian, significant aeolian abrasion and removal of sediments occurred within Gale crater, creating the modern topography that slopes away from Mount Sharp.
7. Aeolian erosion has continued to the present day, leading to the exposure of the Kimberley formation at Windjana from beneath a few meters of overburden at only ~46 Ma.

The geological history implied here has important implications for the past habitability of Gale crater. The Kimberley sediments were deposited near the margins of an ancient, crater-filling lake during the later part of the period when Mars is thought to have had the most favorable conditions for life. The 1 to 4 m stratigraphic thickness of each delta deposit implies a standing body of water of at least that depth for long enough to accumulate the sediment. Based on terrestrial analog rates, *Grotzinger et al.* [2015] estimated that each lake was present for a time span on the order of 100 to 10,000 years, and even as individual lakes came and went, they could have been connected in time through a common groundwater table. Therefore, water may have been continually present within Gale crater for a biologically relevant period of time, albeit under cold climate conditions.

Although detection of organic compounds from the Windjana sample has not been reported, its relatively recent exposure age suggests that, had organics been concentrated during the deposition of the Dillinger member at the Kimberley, they would have been shielded from cosmic ray degradation by a few meters of overburden and likely would have be preserved until ~46 Ma. The absence of organic compounds, however, perhaps is not surprising given that the Dillinger member is a fine-grained sandstone interpreted as a fluvial (or mixed fluvial-aeolian) deposit; organic matter is much more likely to be concentrated in finer-grained facies [e.g., *Summons et al.*, 2011], such as the lacustrine mudstones where organics were detected at Yellowknife Bay [*Freissinet et al.*, 2015], which are not present in the Kimberley formation. During Curiosity's ongoing traverse south through the lower stratigraphy of Mount Sharp, including its current exploration of Murray formation, the rover will characterize mudstones that were deposited in deeper portions of the basin-filling lakes. If ongoing erosion rates at Mount Sharp are similar to those measured at Aeolis Palus, there is a strong possibility that Curiosity can sample a recently exposed outcrop of lacustrine mudstone where organic molecules may have been concentrated and preserved.

Acknowledgments

We acknowledge the exceptional skills and diligent efforts made by the MSL project's science, engineering, and management teams in making this work possible. We are also grateful to the many MSL team members who participated in tactical and strategic operations during the Kimberley campaign. We thank Ryan Anderson and two anonymous reviewers, whose comments have improved the manuscript. Rice was supported by the NASA Astrobiology Institute (NAI) Postdoctoral Program and the MSL Participating Scientist Program. Gupta was supported by grants from the United Kingdom Space Agency (UKSA). Le Deit and Lasue acknowledge the support of the French Space Agency (CNES). Data presented in this paper are archived in the Planetary Data System (pds.nasa.gov).

References

Bandfield, J. L. (2002), Global mineral distributions on Mars, *J. Geophys. Res.*, *107*(E6), 5042, doi:10.1029/2001JE001510.

Baratoux, D., M. Toplis, M. Monnereau, and V. Sautter (2013), The petrological expression of early Mars volcanism, *J. Geophys. Res. Planets*, *118*, 59–64, doi:10.1029/2012JE004234.

Bennett, K. A., and J. F. Bell III (2016), A global survey of Martian central mounds: Central mounds as remnants of previously more extensive large-scale sedimentary deposits, *Icarus*, *264*, 331–341, doi:10.1016/j.icarus.2015.09.041.

Bridges, N. T., et al. (2014), The rock abrasion record at Gale Crater: Mars Science Laboratory results from Bradbury Landing to Rocknest, *J. Geophys. Res. Planets*, *119*, 1374–1389, doi:10.1002/2013JE004579.

Calef, F. J., III, et al. (2013), Geologic mapping of the Mars Science Laboratory landing ellipse, *Lunar Planet Sci.*, *44*, Abstract 2511.

Carter, J., and F. Poulet (2013), Ancient plutonic processes on Mars inferred from the detection of possible anorthositic terrains, *Nat. Geosci.*, *6*(12), 1008–1012.

Day, M., and G. Kocurek (2016), Observations of an aeolian landscape: From surface to orbit in Gale Crater, *Icarus*, *260*, 37–71, doi:10.1016/j.icarus.2015.09.042.

Day, M., W. Anderson, G. Kocurek, and D. Mohrig (2016), Carving intracrater layered deposits with wind on Mars, *Geophys. Res. Lett.*, *43*, 2473–2479, doi:10.1002/2016GL068011.

Delamere, W. A., et al. (2010), Color imaging of Mars by the High Resolution Imaging Science Experiment (HiRISE), *Icarus*, *205*(1), 38–52, doi:10.1016/j.icarus.2009.03.012.

Dow, D. B., and I. Gemuts (1969), Geology of the Kimberley region, Western Australia: East Kimberley, *Bur. Miner. Resour. Aust. Bull.*, *106*.

Edgar, L., et al. (2014), Reconstructing ancient fluvial environments at the Balmville and Dingo Gap outcrops, Gale crater, Mars, Abstract P42C-05 presented at AGU Fall Meeting, San Francisco, Calif.

Fairén, A. G., et al. (2014), A cold hydrological system in Gale crater, Mars, *Planet. Space Sci.*, *93-94*, 101–118.

Farley, K., et al. (2014), In situ radiometric and exposure age dating of the Martian surface, *Science*, *343*(6169), doi:10.1126/science.1247166.

Filiberto, J., and R. Dasgupta (2015), Constraints on the depth and thermal vigor of melting in the Martian mantle, *J. Geophys. Res. Planets*, *120*, 109–122, doi:10.1002/2014JE004745.

Forni, O., et al. (2015a), First detection of fluorine on Mars: Implications for Gale Crater's geochemistry, *Geophys. Res. Lett.*, *42*, 1020–1028, doi:10.1002/2014GL062742.

Forni, O., et al. (2015b), Flourine and lithium at the Kimberley outcrop, Gale Crater, *Lunar Planet Sci.*, *46*, Abstract 1989.

Freissinet, C., et al. (2015), Organic molecules in the Sheepbed Mudstone, Gale Crater, Mars, *J. Geophys. Res. Planets*, *120*, 495–514, doi:10.1002/2014JE004737.

Grant, J. A., S. A. Wilson, N. Mangold, F. Calef III, and J. P. Grotzinger (2014), The timing of alluvial activity in Gale crater, Mars, *Geophys. Res. Lett.*, *41*, 1142–1149, doi:10.1002/2013GL058909.

Grotzinger, J. P. (2014), Habitability, taphonomy, and the search for organic carbon on Mars, *Science*, *343*, 386–387, doi:10.1126/science.1249944.

Grotzinger, J. P., et al. (2012), Mars Science Laboratory mission and science investigation, *Space Sci. Rev.*, *170*(1–4), 5–56.

Grotzinger, J. P., et al. (2014), A habitable fluvio-lacustrine environment at Yellowknife Bay, Gale Crater, Mars, *Science*, *343*(6169, 1,242,777).

Grotzinger, J. P., et al. (2015), Deposition, exhumation, and paleoclimate of an ancient lake deposit, Gale crater, Mars, *Science*, *350*(6257), doi:10.1126/science.aac7575.

Gupta, S., et al. (2014), Making sense of Martian sediments at the Kimberley, Gale crater, Abstract P42C-02 presented at AGU Fall Meeting, San Francisco, Calif.

Johnson, J. R., et al. (2016), Constraints on iron sulfate and iron oxide mineralogy from ChemCam visible/near-infrared reflectance spectroscopy of Mt. Sharp basal units, Gale Crater, Mars, *Am. Min.*, *101*, 1501–1514, doi:10.2138/am20165553.

Kronyak, R. E., L. C. Kah, M. Nachon, N. Mangold, R. C. Weins, R. Williams, J. Schieber, and J. P. Grotzinger (2015), Distribution of mineralized veins from Yellowknife Bay to Mount Sharp, Gale Crater, Mars: Insight from textural and compositional variation, *Lunar Planet Sci.*, *46*, Abstract 1832.

Lanza, N. L., et al. (2016), Oxidation of manganese in an ancient aquifer, Kimberley formation, Gale crater, Mars, *Geophys. Res. Lett.*, *43*, 7398–7407, doi:10.1002/2016GL069109.

Lasue, J., et al. (2016), Observation of $>$ 5 wt % zinc at the Kimberley outcrop, Gale crater, Mars, *J. Geophys. Res. Planets*, *121*, 338–352, doi:10.1002/2015JE004946.

Le Deit, L., E. Hauber, F. Fueten, M. Pondrelli, A. P. Rossi, and R. Jaumann (2013), Sequence of infilling events in Gale Crater, Mars: Results from morphology, stratigraphy, and mineralogy, *J. Geophys. Res. Planets*, *118*, 2439–2473, doi:10.1002/2012JE004322.

Le Deit, L., et al. (2016), The potassic sedimentary rocks in Gale Crater, Mars, as seen by ChemCam on board Curiosity, *J. Geophys. Res. Planets*, *121*, 784–804, doi:10.1002/2015JE004987.

Litvak, M. L., et al. (2016), Hydrogen and chlorine abundances in the Kimberley formation of Gale crater measured by the DAN instrument on board the Mars Science Laboratory Curiosity rover, *J. Geophys. Res. Planets*, *121*, 836–845, doi:10.1002/2015JE004960.

Malin, M. C., and K. S. Edgett (2000), Sedimentary rocks of early Mars, *Science*, *290*, 1927, doi:10.1126/science.290.5498.1927.

Mangold, N., et al. (2016), Composition of conglomerates analyzed by the Curiosity rover: Implications for Gale Crater crust and sediment sources, *J. Geophys. Res. Planets*, *121*, 353–387, doi:10.1002/2015JE004977.

McLennan, S. M., et al. (2014), Elemental geochemistry of sedimentary rocks at Yellowknife Bay, Gale Crater, Mars, *Science*, *343*(6169), doi:10.1126/science.1244734.

Nachon, M., et al. (2014), Calcium sulfate veins characterized by ChemCam/Curiosity at Gale Crater, Mars, *J. Geophys. Res. Planets*, *119*, 1991–2016, doi:10.1002/2013JE004588.

Oehler, D. Z., et al. (2016), Origin and significance of decameter-scale polygons in the lower Peace Vallis fan of Gale crater, Mars, *Icarus*, *277*, 56–72.

Palucis, M. C., et al. (2014), The origin and evolution of the Peace Vallis fan system that drains to the Curiosity landing area, Gale Crater, Mars, *J. Geophys. Res. Planets*, *119*, 705–728, doi:10.1002/2013JE004583.

Rogers, A. D., and H. Nekvasil (2015), Feldspathic rocks on Mars: Compositional constraints from infrared spectroscopy and possible formation mechanisms, *Geophys. Res. Lett.*, *42*, 2619–2626, doi:10.1002/2015GL063501.

Rogers, A. D., and V. E. Hamilton (2015), Compositional provinces of Mars from statistical analyses of TES, GRS, OMEGA and CRISM data, *J. Geophys. Res. Planets*, *120*, 62–91, doi:10.1002/2014JE004690.

Rubin, D., et al. (2015), Sedimentary facies as indicators of changing lake levels in Gale crater, Mars, Abstract P43B-2116 presented at AGU Fall Meeting, San Francisco, Calif.

Santos, A. R., et al. (2015), Petrology of igneous clasts in Northwest Africa 7034: Implications for the petrologic diversity of the Martian crust, *Geochim. Cosmochim. Acta*, *157*, 56–85.

Sautter, V., et al. (2014), Igneous mineralogy at Bradbury Rise: The first ChemCam campaign at Gale crater, *J. Geophys. Res. Planets*, *119*, 30–46, doi:10.1002/2013JE004472.
Sautter, V., et al. (2015), In situ evidence for continental crust on early Mars, *Nat. Geosci.*, doi:10.1038/NGEO2474.
Sautter, V., et al. (2016), Magmatic complexity on early Mars as seen through a combination of orbital, in-situ and meteorite data, *Lithos*, *254–255*, 36–52, doi:10.1016/j.lithos.2016.02.023.
Schieber, J., et al. (2016), Encounters with an unearthly mudstone: Understanding the first mudstone found on Mars, *Sedimentology*, doi:10.1111/sed.12318.
Serventi, G., et al. (2013), Spectral variability of plagioclase–mafic mixtures (1): Effects of chemistry and modal abundance in reflectance spectra of rocks and mineral mixtures, *Icarus*, *226*(1), 282–298, doi:10.1016/j.icarus.2013.05.041.
Siebach, K. L., et al. (2015), Sorting out APXS compositional variations in Gale crater sedimentary rocks, Mars, Abstract 94-2 presented at GSA Annual Meeting, Baltimore, Md.
Stack, K. M., et al. (2014), Diagenetic origin of nodules in the Sheepbed member, Yellowknife Bay formation, Gale crater, Mars, *J. Geophys. Res. Planets*, *119*, 1637–1664, doi:10.1002/2014JE004617.
Stack, K. M., et al. (2016), Comparing orbiter and rover image-based mapping of an ancient sedimentary environment, Aeolis Palus, Gale Crater, Mars, *Icarus*, *280*, 3–21, doi:10.1016/j.icarus.2016.02.024.
Stolper, E. M., et al. (2013), The petrochemistry of Jake_M: A Martian mugearite, *Science*, *341*(6153), doi:10.1126/science.1239463.
Summons, R. E., et al. (2011), Preservation of Martian organic and environmental records: Final report of the Mars biosignature working group, *Astrobiology*, *11*(2), 157–181.
Szabó, T., D. Gábor, J. P. Grotzinger, and D. J. Jerolmack (2015), Reconstructing the transport history of pebbles on Mars, *Nat. Commun.*, *6*, 8366, doi:10.1038/ncomms9366.
Taylor, S. R., and S. M. McLennan (2009), *Planetary Crusts: Their Composition, Origin and Evolution*, Cambridge Univ. Press, Cambridge, U. K.
Thompson, L. M., et al. (2016), Potassium-rich sandstones within the Gale impact crater, Mars: The APXS perspective, *J. Geophys. Res. Planets*, *121*, 1981–2003, doi:10.1002/2016JE005055.
Thomson, B. J., et al. (2011), Constraints on the origin and evolution of the layered mound in Gale Crater, Mars using Mars Reconnaissance Orbiter data, *Icarus*, *214*(2), 413–432.
Treiman, A. H., and E. Medard (2016), Mantle metasomatism in Mars: Potassic basaltic sandstone in Gale crater derived from partial melt of phlogopite-peridotite, Abstract 49-12 presented at GSA Annual Meeting, Denver, Colo.
Treiman, A. H., et al. (2016), Mineralogy, provenance, and diagenesis of a potassic basaltic sandstone on Mars: CheMin X-ray diffraction of the Windjana sample (Kimberley area, Gale crater), *J. Geophys. Res. Planets*, *121*, 75–106, doi:10.1002/2015JE004932.
Tyler, I. M., R. M. Hocking, and P. W. Haines (2012), Geological evolution of the Kimberley region of Western Australia, *Episodes*, *35*, 298–306.
Vasavada, A. R., et al. (2014), Overview of the Mars Science Laboratory mission: Bradbury Landing to Yellowknife Bay and beyond, *J. Geophys. Res. Planets*, *119*, 1134–1161, doi:10.1002/2014JE004622.
Vasconcelos, P. M., et al. (2016), Discordant K-Ar and concordant exposure dates for the Windjana sandstone, Kimberley, Gale crater, Mars, *J. Geophys. Res. Planets*, *121*, 2176–2192, doi:10.1002/2016JE005017.
Wellington, D., et al. (2016), Visible to near-infrared MSL/Mastcam multispectral imaging: Initial results from select high-interest science targets within Gale crater, Mars, *Am. Min.*, doi:10.2138/am-2017-5760CCBY, in press.
Williams, R. M. E., et al. (2013), Martian fluvial conglomerates at Gale crater, *Science*, *340*, 1068–1072, doi:10.1126/science.1237317.
Williams, R. M. E., et al. (2015), Unraveling Curiosity observations of sedimentary rocks at Kylie, *Lunar Planet Sci.*, *46*, Abstract 2385.
Wittmann, A., et al. (2015), Petrography and composition of Martian regolith breccia meteorite northwest Africa 7475, *Meteorit. Planet. Sci.*, *50*, 326–352.
Wray, J. J., S. T. Hansen, J. Dufek, G. A. Swayze, S. L. Murchie, F. P. Seelos, J. R. Skok, R. P. Irwin III, and M. S. Ghiorso (2013), Prolonged magmatic activity on Mars inferred from the detection of felsic rocks, *Nat. Geosci.*, *6*(12), 1013–1017.